PALEOCEANOGRAPHY, VOL. 13, NO. 3, PAGES 298-310, JUNE 1998

Global deep-sea burial rate of calcium carbonate during the last glacial maximum

Nina R. Catubig,[1,2] D. E. Archer,[1] Roger Francois,[3] Peter deMenocal,[4]
Will Howard,[5] Ein-Fen Yu[6]

Abstract. Global databases of calcium carbonate concentrations and mass accumulation rates in Holocene and last glacial maximum sediments were used to estimate the deep-sea sedimentary calcium carbonate burial rate during these two time intervals. Sparse calcite mass accumulation rate data were extrapolated across regions of varying calcium carbonate concentration using a gridded map of calcium carbonate concentrations and the assumption that accumulation of noncarbonate material is uncorrelated with calcite concentration within some geographical region. Mean noncarbonate accumulation rates were estimated within each of nine regions, determined by the distribution and nature of the accumulation rate data. For core-top sediments the regions of reasonable data coverage encompass 67% of the high-calcite (>75%) sediments globally, and within these regions we estimate an accumulation rate of $55.9 \pm 3.6 \times 10^{11}$ mol yr^{-1}. The same regions cover 48% of glacial high-$CaCO_3$ sediments (the smaller fraction is due to a shift of calcite deposition to the poorly sampled South Pacific) and total $44.1 \pm 6.0 \times 10^{11}$ mol yr^{-1}. Projecting both estimates to 100 % coverage yields accumulation estimates of 8.3×10^{12} mol yr^{-1} today and 9.2×10^{12} mol yr^{-1} during glacial time. This is little better than a guess given the incomplete data coverage, but it suggests that glacial deep sea calcite burial rate was probably not considerably faster than today in spite of a presumed decrease in shallow water burial during glacial time.

1. Introduction.

The ocean cycle of calcium carbonate ($CaCO_3$) consists of a balance between the supply of calcium (Ca^{2+}) ions and carbonate alkalinity (HCO_3^- and $CO_3^=$) to the oceans from chemical weathering of the continents and burial in the deep sea and in shallow waters. Deep-sea burial of $CaCO_3$, predominantly as the mineral calcite, is controlled by the rate of $CaCO_3$ production by pelagic plankton and by the saturation state of the deep waters with respect to calcite. An increase in ocean [$CO_3^=$] depresses the depth of calcite saturation and increases the seafloor surface area upon which calcite preservation occurs. Therefore an imbalance between weathering and burial of $CaCO_3$ drives ocean [$CO_3^=$] in the direction of reconciling the imbalance, making ocean $CaCO_3$ a slave to weathering rates on timescales of 5-10 kyr [*Broecker and Peng*, 1982; *Boyle*, 1988; *Emerson and Archer*, 1992; *Archer et al.*, 1997].

[1]Department of Geophysical Sciences, University of Chicago, Chicago, Illinois.
[2]Now at Museum of Science, Boston , Massachusetts.
[3]Woods Hole Oceanographic Institution, Woods Hole, Massachusetts
[4]Lamont-Doherty Earth Observatory, Palisades, New York.
[5]Antarctic Cooperative Research Center, University of Tasmania, Hobart, Tasmania, Australia.
[6]Department of Earth Sciences, National Taiwan Normal University, Taipei, Taiwan.

Copyright 1998 by the American Geophysical Union.

Paper number 98PA00609.
0883-8305/98/98PA00609$12.00

An estimate of deep-sea calcite burial provides a constraint on how the carbon cycle responds to glacial/interglacial climate cycles. Since the ocean and atmosphere are interdependent, understanding the changes in the ocean during the last glacial maximum (LGM) should shed some light on the mechanism by which atmospheric CO_2 responds to the glacial cycles [*Berger*, 1982; *Keir and Berger*, 1985; *Opdyke and Walker*, 1992]. Today, the rate of shallow ocean $CaCO_3$ burial is estimated to be roughly equal in magnitude to the rate of burial in the deep sea today, and because of the exposure of the continental shelves by lowered LGM sea level, it is generally believed that that shallow water deposition was considerably lower during LGM [*Milliman*, 1974]. On the timescale of $CaCO_3$ compensation both of these effects should have driven a deepening of the lysocline during glacial time and an increase in deep-sea calcite burial; in the steady state limit we would expect an LGM $CaCO_3$ burial rate which exceeds the present-day value by as much as a factor of 2. An estimate of the rate of deep-sea $CaCO_3$ deposition during LGM should provide a direct test of these ideas.

Calcite concentration data from glacial time are much more numerous than are calcite accumulation rate data. Also, much of the spatial variability in calcite accumulation rate is driven by variability in dissolution and preservation of calcite with depth in the ocean (the calcite lysocline). Therefore we develop a method for extending the relatively sparse accumulation rate data across variations in calcite concentration by normalizing the accumulation rate data to the noncalcite component and taking regional averages. Calcite accumulation rates are then calculated from gridded fields of calcite concentration and regional averages of the noncalcite accumulation rate.

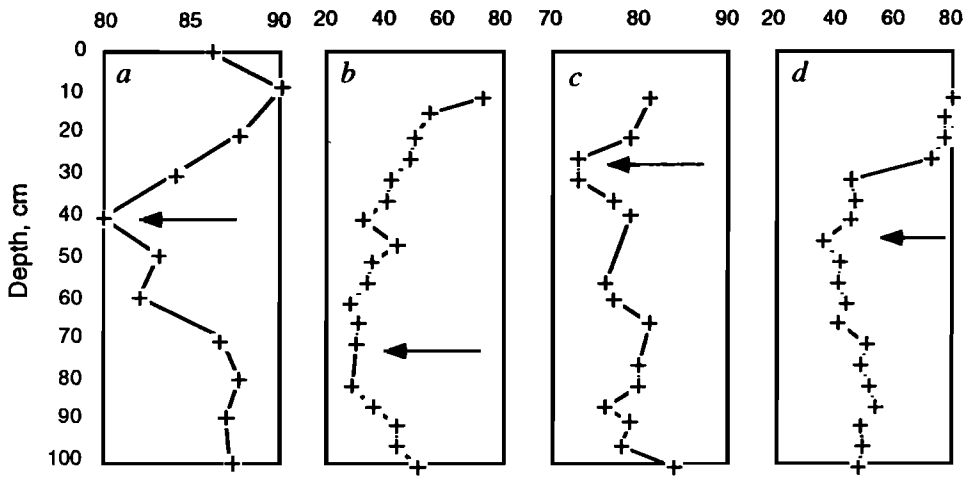

Figure 1. Downcore calcite concentration profiles used to correlate to (a) RC12-225 [*Luz*, 1977; *Burkle et al.*, 1978], b) RC8-89, c) RC8-92, and d) RC12-227. to determine the depth of the last glacial maximum (LGM) (arrow).

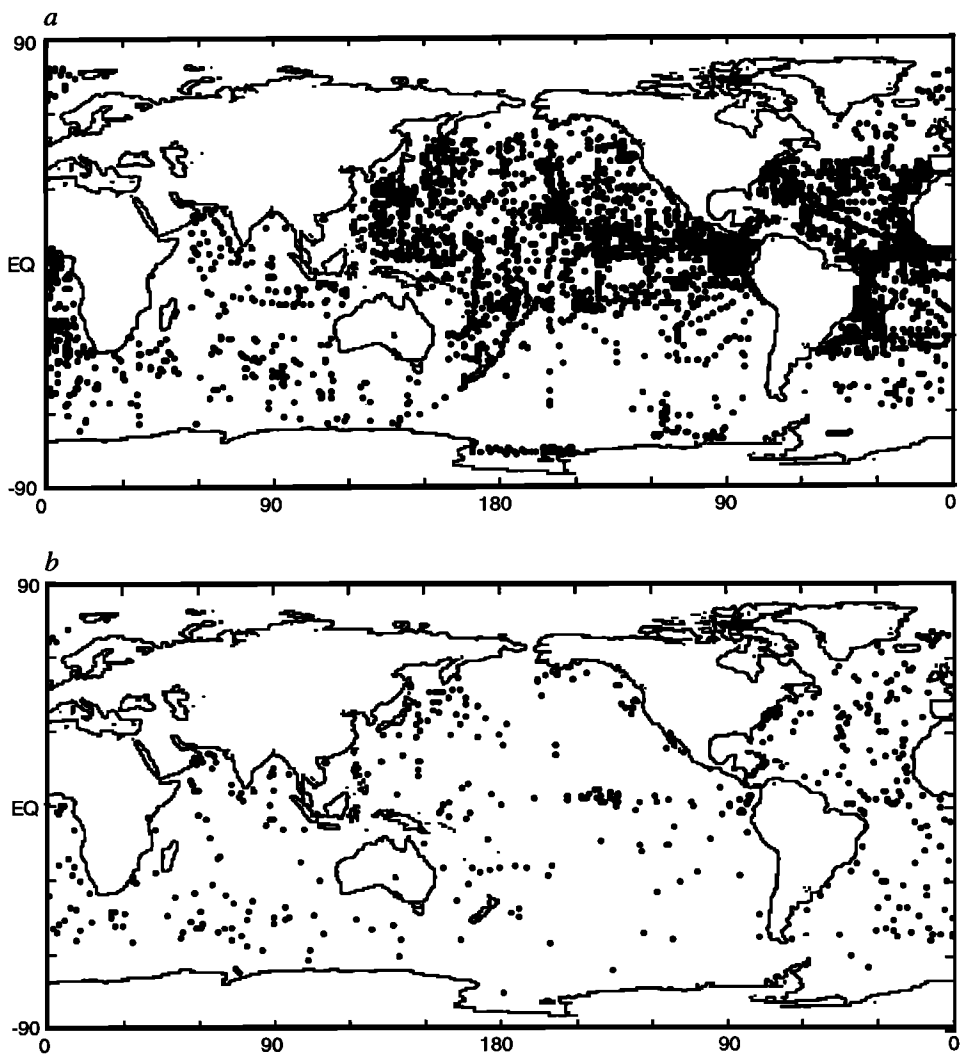

Figure 2. Percent calcite data locations: (a) core top and (b) LGM. Most cores in both data sets are located in the Atlantic and Pacific Oceans. Coverage of the Indian and Southern Oceans (especially the Pacific sector of the Southern Ocean) is poor.

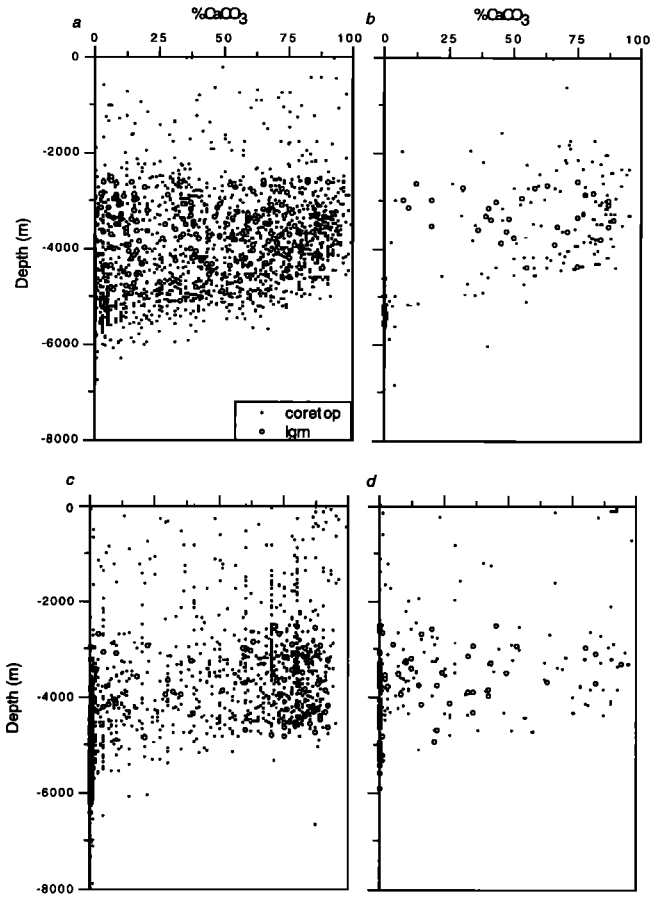

Figure 3. Values of $\%CaCO_3$ versus depth for the (a) Atlantic, (b) Indian, (c) Pacific, and (d) Southern Oceans. The small number of LGM data points makes it difficult to see if the lysocline changed between the LGM and today.

2. Data Sources

2.1. $CaCO_3$ Concentration

Core-top $\%CaCO_3$ data were discussed by Archer [1996]. LGM $\%CaCO_3$ data presented in Appendix A1[1] come from a variety of sources [*Broecker and Takahashi*, 1966; *McManus et al.*, 1970; *Burns et al.*, 1973; *Creager et al.*, 1973; *Heezen et al.*, 1973; *Luz and Shackleton*, 1973; *von der Borch et al.*, 1974; *Davies et al.*, 1974; *Andrews et al.*, 1975; *Hayes et al.*, 1975; *Karig et al.*, 1975; *Larson et al.*, 1975; *Hays et al.*, 1976; *Morley and Hays*, 1979; *Moore et al.*, 1980; *Hussong et al.*, 1981; *Cooke and Hays*, 1982; *Heath et al.*, 1982; *Leinen*, 1985; *Peterson and Prell*, 1985; *Cwienk*, 1986; *Balsam and McCoy*, 1987; *Barker et al.*, 1988; *Ciesielski et al.*, 1988; *Lyle et al.*, 1988; *Barron et al.*, 1989; *Droxler et al.*, 1990; *Farrell*, 1990; *Prell et al.*, 1990; *Yang et al.*, 1990; *Bareille*, 1991; *Broecker et al.*, 1991; *Steens et al.*, 1991; *Zahn and Peterson*, 1991; *Howard and Prell*, 1992; *Karlin et al.*, 1992; *Keigwin et al.*, 1992; *Lyle et al.*, 1992; *Mackensen et al.*, 1992*Howard and Prell*, 1994; *Snoeckx and Rea*, 1994; *LaMontagne et al.*, 1996; *Lynch-Steiglitz et al.*, 1996; *Oritz et al.*, 1997] either previously published $\%CaCO_3$ values or dated cores which could be analyzed for calcite concentration. LGM is defined as $\partial^{18}O$ stage 2 [*Imbrie et al.* 1984], identified by one or several of the following methods: oxygen isotope stratigraphy, calcium carbonate stratigraphy, ^{14}C dating, foraminiferal biostratigraphy, or lithologic stratigraphy. The depth of the LGM level in 56 Climate: Long-Range Investigation, Mapping, and Prediction (CLIMAP) cores was identified but no $\%CaCO_3$ value was published [*Biscaye et al.*, 1976, *Hays et al.*, 1976, *Kolla et al.*, 1976; *Moore et al.*, 1980; *Cooke et al.*, 1982], so we collected samples from the Lamont-Doherty core archives and measured $\%CaCO_3$ by coulometry. Cores with no measurable $CaCO_3$ to a depth of 50 cm were entered into the LGM data set as containing 0% $CaCO_3$. We also determined the downcore calcium carbonate stratigraphy for three cores in the East Pacific Rise and southwest Pacific where data coverage was particularly weak, estimating the depth to LGM by correlating the $\%CaCO_3$ stratigraphy to RC12-225 [*Luz*, 1977; *Burkle et al.*, 1978; *Howard and Prell*, 1994] (Figure 1). We have 3712 $\%CaCO_3$ core-top values and 472 LGM values (Figure 2). The Atlantic Ocean is well covered by both the LGM and the core-top data; data in the Pacific and Indian Oceans are scattered, with better coverage from the core-top than the LGM. Plots of $\%CaCO_3$ versus depth (Figure 3) are difficult to distinguish between the core top and LGM because of scatter in the data. A more sensitive diagnostic is a direct point-by-point comparison of $\%CaCO_3$ values for cores where both values are available (Figure 4). Most of the data in the Southern and Atlantic Oceans fall on the side of higher core-top relative to LGM $\%CaCO_3$ values, whereas the majority of the Pacific data points fall on the side of low values. Data in the Indian Ocean are insufficient to allow a determination. These observations are consistent with the idea that calcite preservation in the Pacific is out-of-phase with the rest of the oceans [*Arrhenius*, 1952; *Berger*, 1973; *Farrell and Prell*, 1989].

2.2. Mass Accumulation Rates

Mass accumulation rate (MAR) data were assembled from many sources [*Berger et al.* 1976; *Biscaye et al.* 1976; *Kolla et al.* 1976; *Luz*, 1977; *Moore et al.*, 1980; *Berger and Killingly*, 1982; *Kent*, 1982; *Morley and Shackleton*, 1984; *Leinen*, 1985; *Curry and Lohmann*, 1986; *Cwienk*, 1986; *Balsam*, 1988; *Curry and Lohmann*, 1990; *Farrell*, 1990; *Charles et al.*, 1991; *Francois and Bacon*, 1991; *Mortlock et al.*, 1991; *Rea et al.*, 1991; *Keigwin et al.*, 1992; *Cremer et al.*, 1993; *Murray et al.*, 1993; *Howard and Prell*, 1994; *Yu*, 1994] (Appendix A-2). Accumulation rates were determined by ^{14}C dating, ^{230}Th mass balance, and calcium carbonate, $\partial^{18}O$, and faunal stratigraphies. Accumulation rates based on ^{14}C may be biased because of the deviation of the ^{14}C timescale from the real calendar, which could offset the accumulation rate by up to 20%. Sediment focusing can also offset local accumulation rates from regional averages, with a potential for postitive bias if cores are preferentially taken from local valleys where sedimentation is more likely to be continuous. No attempt has been made to correct for these potential biases; rather we look to a repetition of the

[1]Appendices A1 and A2 are available electronically at the National Geophysical Data Center, Boulder, Colo. (URL: http://www.ngdc.noaa.gov).

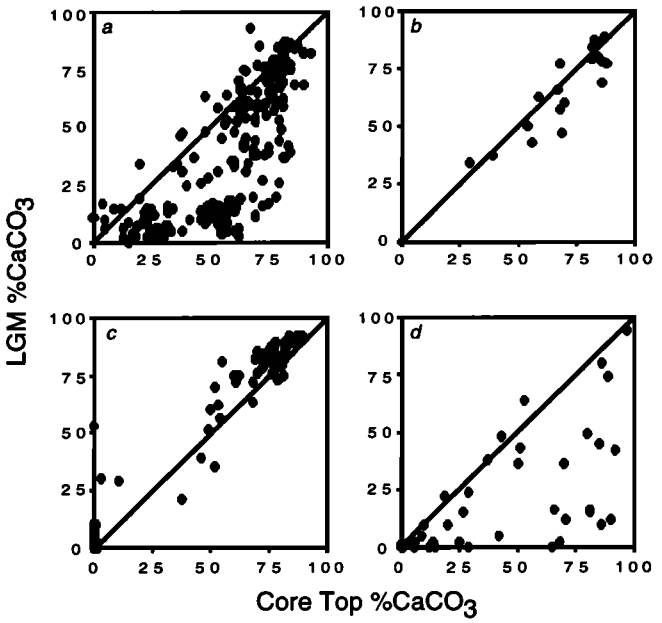

Figure 4. Percent calcite plots, core top versus LGM: (a) Atlantic, (b) Indian, (c) Pacific, and (d) Southern Oceans. We compare LGM and core-top percent calcite data from cores for which both measurements are available. The solid line denotes a 1:1 relationship. Most of the data clusters around this line, but there is a tendency toward higher core-top percent calcite values in all of the oceans except for the Pacific Ocean. The cluster of data in the Atlantic Ocean with LGM percent calcite values lower than 25% is from the North Atlantic where changes in ice-rafted debris are responsible for the large changes in percent calcite values.

calculation in the future as more ^{230}Th accumulation rate data become available. Core-top data are available from each of the major ocean basins, but they are not evenly distributed. In particular, data are sorely needed in the South Pacific Ocean (Figure 5).

3. Methods

The accumulation rate of $CaCO_3$ depends strongly on the extent of seafloor dissolution, which varies as a function of depth in the ocean (generating the calcite lysocline). Sedimentary $\%CaCO_3$ data coupled with the ocean bathymetry are abundant enough to resolve the distribution of $CaCO_3$ fairly well, in the form of gridded maps of $\%CaCO_3$ for present-day and LGM. Accumulation rate data, on the other hand, are too sparse to resolve variations across the lysocline, and the strategy we take to generalize the MAR data is as follows. Calcite-derived variations in MAR are removed from the data set by normalizing to a calcite-free (non-$CaCO_3$) basis and averaged to estimate regional mean non-$CaCO_3$ MAR. The rate of $CaCO_3$ accumulation as controlled by variations in $CaCO_3$ concentration (the lysocline) are then estimated using

$$\text{Calcite MAR}\left(\frac{\text{g}}{\text{cm}^2\,\text{kyr}}\right) = \text{regional non-CaCO}_3\text{ MAR} \times \frac{\%CaCO_3}{100 - \%CaCO_3} \quad (1)$$

where the $\%CaCO_3$ value is derived from the gridded $\%CaCO_3$ map. This expression is based on what we will refer to as the "constant dilution assumption" that $\%CaCO_3$ can be used as an indicator for $CaCO_3$ MAR using a regionally uniform non-$CaCO_3$ MAR. The calculation therefore requires a regional average value of the non-$CaCO_3$ MAR and a gridded field of $\%CaCO_3$ which resolves the calcite lysocline.

3.1. Regional Average Noncarbonate Accumulation Rates

We define 10 basin-scale regions where MAR data appear to be sufficient for analysis (Table 1 and Figure 5): the northwest Atlantic, northeast Atlantic, tropical Atlantic, South Atlantic, Indian, North Pacific, equatorial Pacific, north equatorial Pacific, western tropical Pacific, and the Southern Ocean. As explained above, we will assume that a single non-$CaCO_3$ MAR can be used to approximate the value at each grid point in the domain so that $\%CaCO_3$ can be used to estimate $CaCO_3$ MAR: the constant dilution assumption. This assumption would break down, leading to spurious regional MAR estimates, if the non-$CaCO_3$ MAR varies so widely that it affects $\%CaCO_3$ by variable dilution. These two scenarios can be distinguished by looking for a correlation between $\%CaCO_3$ and the non-$CaCO_3$ MAR (Figure 6). Data from shallower than 2500 m were excluded from consideration in all regions. In most of the regions the remaining non-$CaCO_3$ MAR are scattered but uncorrelated with $\%CaCO_3$, supporting the constant dilution assumption. In the northwest Atlantic, however, we observe a systematic trend toward high noncarbonate MAR in low-calcite sediments, suggesting that dilution influences $\%CaCO_3$. Therefore we exclude the north Atlantic from further consideration. Three data points in the LGM tropical Atlantic show high non-$CaCO_3$ MAR at low $\%CaCO_3$; we will continue with the calculation from region but will treat the results with caution. Out of a total of 349 core-top mass accumulation rate estimates in our database we utilize 191 for the constant dilution calculation, and we utilize 86 out of a total of 107 available for LGM. A latitudinal trend in non-$CaCO_3$ accumulation away from the equator in the eastern tropical Pacific motivated the split into equatorial, north tropical, and western tropical Pacific boxes. Latitudinal variation in opal burial in the Southern Ocean required that we base the analysis from this region on the noncarbonate, nonopal MAR (Appendix A-2).

In general, histograms of the distributions of calcite MAR data correlate with expected calcite MAR values based on the gridded $\%CaCO_3$ maps and the constant dilution assumption (Figure 7). However, there are regions (e.g., the Southern Ocean and the South Atlantic) where the calcite MAR data vary widely because of variability in the noncarbonate accumulation rate. Regional average noncarbonate accumulation rates are higher today than during glacial time in the tropical and South Atlantic and the Southern Ocean, and lower in the Northeast Atlantic and throughout the Pacific Ocean (Table 2).

3.2. Gridded Maps of Calcite Concentration.

The other required ingredient for calculating regionally integrated calcite burial rates is an estimate of the area in each region covered by high-$\%CaCO_3$ sediments. This we accomplish using the regional $\%CaCO_3$/depth relationship

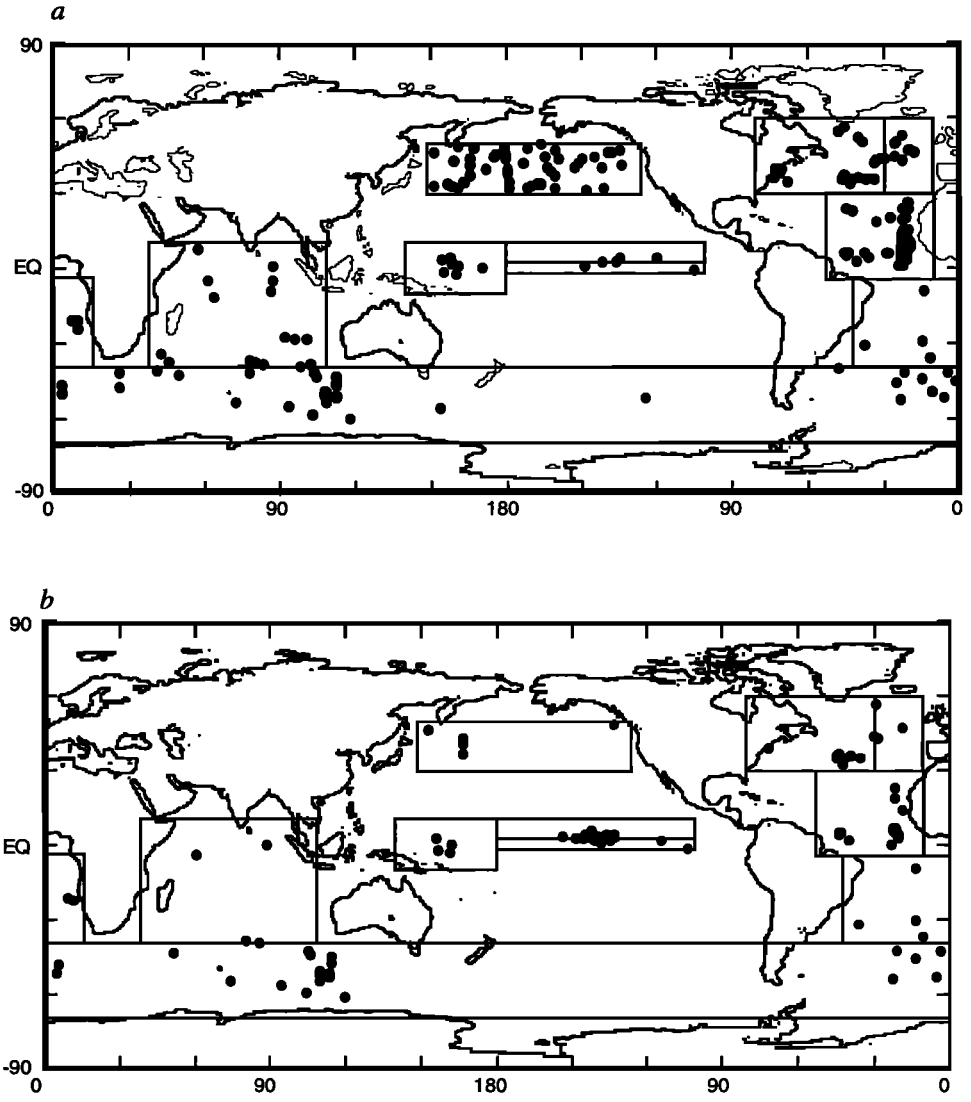

Figure 5. Mass accumulation rate data locations: (a) core top and (b) LGM. Mass accumulation rate data are very sparse in number, but the core-top data are spread out more than the very localized LGM data There is better coverage of the oceans by the core-top data than by the LGM data.

Table 1. Regions of the Global Ocean for Integration of $CaCO_3$ Mass Accumulation Rate (MAR)

Region	Latitude	Longitude	Area, 10^6 km^2
NW Atlantic	30-60°N	80-30°W	13.07
NE Atlantic	30-60°N	30-10°W	5.64
Tropical Atlantic	5°S-30°N	10-50°E	17.60
South Atlantic	5-40°S	50°W-15°E	27.20
Indian Ocean	10°N-40°S	40-90°E	30.15
North Pacific	30-50°N	150°E - 125°W	17.07
Equatorial Pacific	2°N-2°S	180°-100°W	6.26
North Equatorial Pacific	10-2°N	180°-100°W	10.09
Western Tropical Pacific	10°N-10°S	140°E-180°	10.62
Southern Ocean	40-70°S	circum.	78.69

and a gridded field of the ocean bathymetry (from ETOPO-5) to generate a gridded field of predicted $\%CaCO_3$ values. The gridding algorithm for core-top data was presented by Archer [1996]. Gridded $\%CaCO_3$ values were interpolated in depth from ungridded data that fell within three-dimensional ellipsoids of the target point in latitude, longitude, and depth. For the core-top map the latitudinal sizes of the ellipsoids ranged from ±5° at the equator to ±15° at high latitudes (to allow for equatorial heterogeneity) ±15°cos(latitude) longitudinally (to maintain constant width in kilometers), and ±1000 m depth. The LGM data were processed using the same gridding algorithm but with larger ellipsoids, which ranged in latitude from ± 8° at the equator to ±25° in high latitudes, and ±25°cos(latitude) longitudinally, and ±2000 m depth. For the core-top data set the method is able to predict each of the data points with an rms error of 13.5%. The error for the LGM is 22%; higher than the core-top error because of the

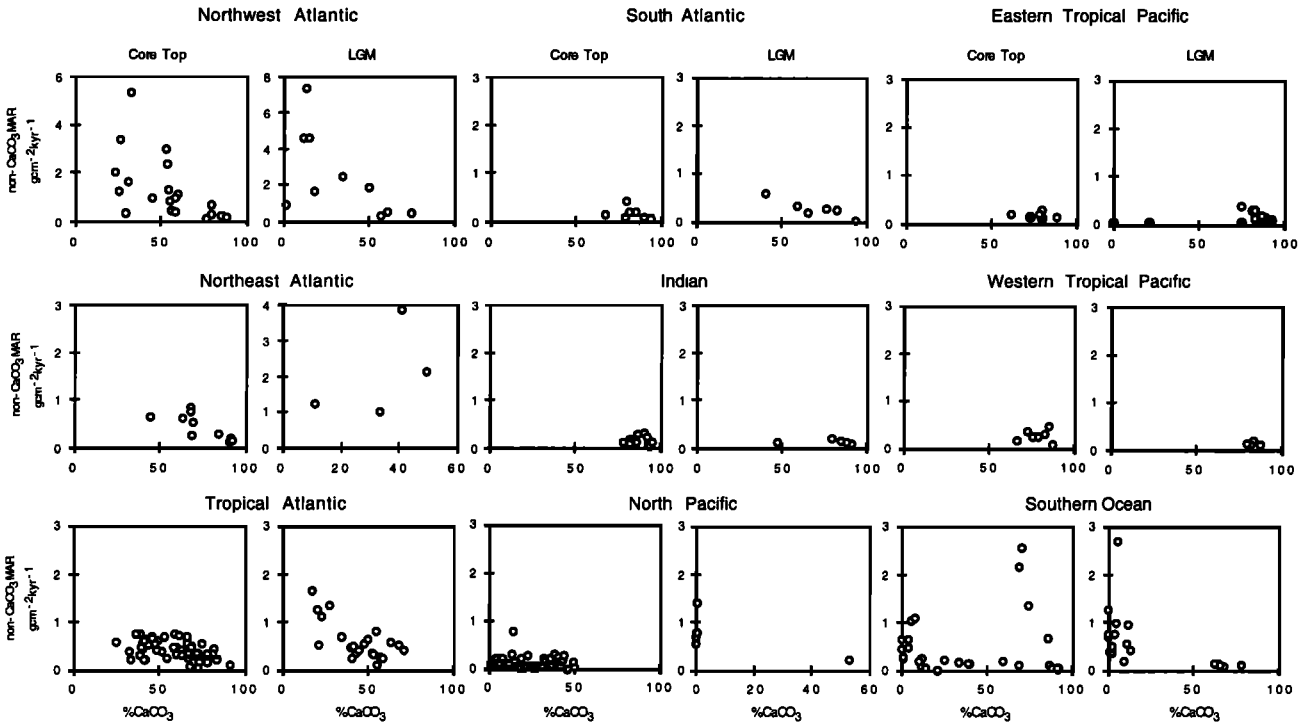

Figure 6. Noncarbonate accumulation rates versus percent calcite by region In the Southern Ocean we show both noncarbonate and nonbiogenic accumulation rates. The nonbiogenic accumulation rates are more constant over the region so we use these to estimate the calcite accumulation rates in the Southern Ocean (under the constant dilution assumption.) Noncarbonate mass accumulation rates (MAR) in the northwest Atlantic are variable and correlated to $\%CaCO_3$, which implies that the distribution of calcite is determined in some part by dilution Therefore we exclude this region from our analysis.

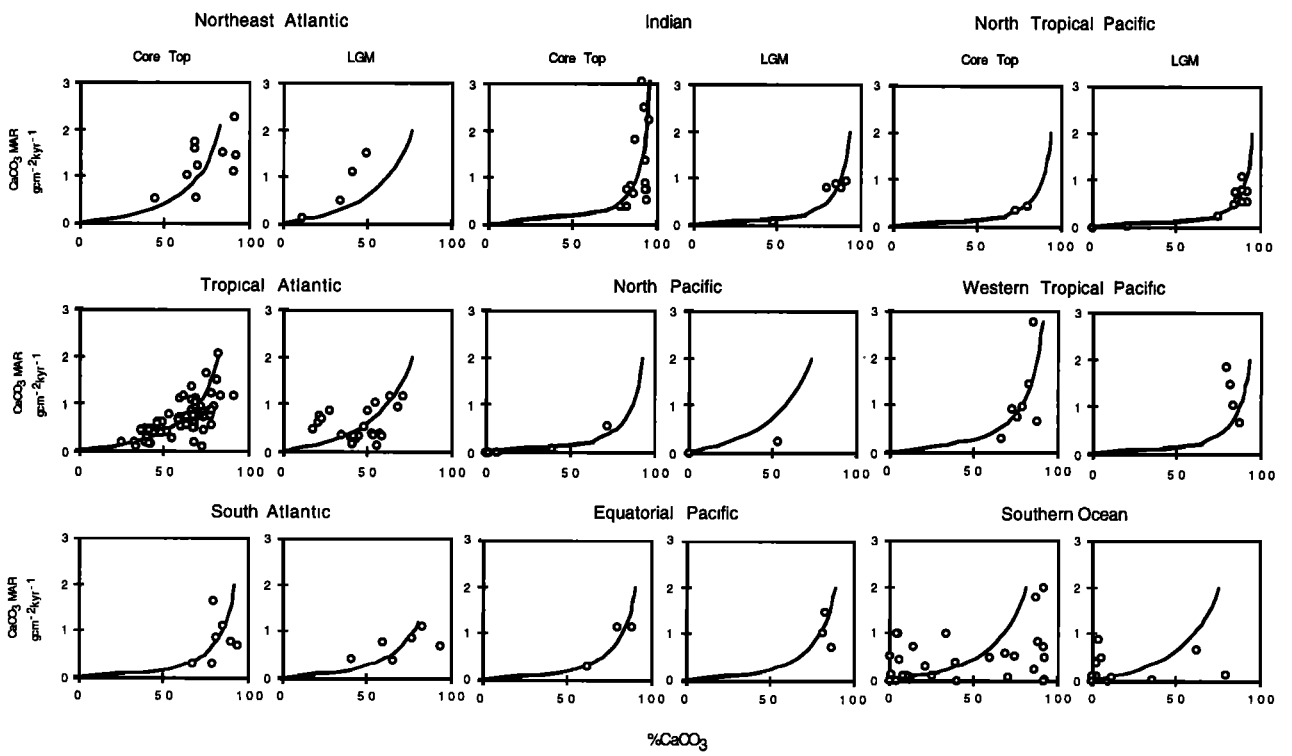

Figure 7. The relationship between $\%CaCO_3$ and $CaCO_3$ MAR, from data (circles) and from the constant-dilution assumption and the regional average non-$CaCO_3$ MAR value (Table 1) (lines). The maximum $CaCO_3$ MAR value is indicated by the lines, and is taken to be 2.0 g cm^{-2} kyr^{-1}, or the maximum observed value in the data, whichever is higher.

Table 2. Statistics of Regional Average Non-$CaCO_3$ MAR Values

Region	Holocene				Last Glacial Maximum			
	Mean Non-$CaCO_3$ MAR[a]	Maximum CMAR[a]	n	Relative Confidence Limits	Mean Non-$CaCO_3$ MAR[a]	Maximum CMAR[a]	n	Relative Confidence Limits
NE Atlantic	0.44	2.3	10	44%	2.06	2.0	4	100%
Tropical Atlantic	0.42	2.5	65	11%	0.61	2.0	23	28%
South Atlantic	0.17	2.0	7	69%	0.28	2.0	6	67%
Indian Ocean	0.13	3.1	14	36%	0.13	2.0	5	43%
North Pacific	0.15	2.0	47	27%	0.73	2.0	5	73%
Equatorial Pacific	0.21	2.0	4	45%	0.25	2.0	6	43%
North Equatorial Pacific	0.13	2.0	2	86%	0 09	2.0	11	21%
Western Tropical Pacific	0.27	2.0	7	43%	0 14	2.0	4	45%
Southern Ocean	0.47	2.0	35	56%	0.64	2.0	22	42%

[a]Non-$CaCO_3$ MAR and $CaCO_3$ MAR (CMAR) in units of g cm^{-2} kyr^{-1}.

sparser $\%CaCO_3$ data for LGM. A Monte Carlo method was used to derive the best gridded $\%CaCO_3$ data given the uncertainty in ungridded $\%CaCO_3$ data (see below).

The maps generated by gridding (Figure 8) reveal high present-day and low LGM $\%CaCO_3$ values in the Atlantic, Indian, and Southern Oceans, low present-day and high LGM $\%CaCO_3$ values in the Pacific consistent with previous compilations [*Berger et al.*, 1976; *Biscaye et al.*, 1976; *Kolla et al.*, 1976; *Morley and Hays*, 1979; *Balsam*, 1981; *Peterson and Prell*, 1985; *Farrell and Prell*, 1989; *Bareille*, 1991 We see that the "polar sedimentary front" (the transition from high to low $\%CaCO_3$ sediments in the Southern Ocean) moved northward during LGM. We compared the gridded and ungridded $\%CaCO_3$ data and found that in most areas the ungridded $\%CaCO_3$ data resemble the gridded product in their distribution (Figure 9). To the extent that the gridded field contains, for example, fewer high-$CaCO_3$ data points than the ungridded data from that region, we conclude that the ungridded data were more plentiful in shallower waters. This can be seen most particularly in the South Atlantic and the glacial equatorial Pacific. The observation percentages in the gridded values do not sum to 100% because of areas of missing data.

3.3. Regional Calcite Accumulation Rates

Regional average calcite MAR was estimated by adding the results of the constant dilution method over each grid point of the gridded $\%CaCO_3$ field. Histograms of the gridded calcite MAR estimates differ somewhat from those of the ungridded MAR data because of the scarcity of the data (Figure 10). However, the gridded values also incorporate information from the gridded $\%CaCO_3$ map, which is based on greater data density. A particular weakness of the constant dilution method is that the uncertainty in the calcite accumulation rate increases greatly as $\%CaCO_3$ approaches 100, so that an error in the high range of $\%CaCO_3$ will be amplified when it is used to calculate calcite MAR. To counter this, we capped the inferred $CaCO_3$ MAR in the gridded field at a value of 2.0 g cm^{-2} kyr^{-1}, or the highest calcite accumulation value observed in the region, whichever is higher (Table 2).

3.4. Uncertainty in Regional Calcite Accumulation Rate

Uncertainty in the estimates of regional MAR stem from at least two sources: the ungridded $\%CaCO_3$ data from which the gridded maps were derived and the mean value of the non-$CaCO_3$ accumulation rate. Since the regional $CaCO_3$ MAR is the product of non-$CaCO_3$ MAR times a function of the $\%CaCO_3$ field (essentially the factor g $CaCO_3$ g^{-1} non-$CaCO_3$) we can calculate the uncertainties in these two pieces separately and then combine them.

The complicated dependence of each gridded $\%CaCO_3$ value on the ungridded data and the nonlinear dependence of the accumulation rate estimate on the gridded $\%CaCO_3$ make it challenging to assess the uncertainty in regional MAR estimates due to the $\%CaCO_3$ field. We used a Monte Carlo method which allowed random noise in the ungridded $\%CaCO_3$ data to generate noise in the gridded maps. For each of 100 trials a random uncorrelated component of noise was added to each ungridded $\%CaCO_3$ value in the data set. The amplitude of the noise imposed on the ungridded data was taken from the accuracy with which the gridding method is able to reproduce the observed $\%CaCO_3$ data. For each trial, the ungridded $\%CaCO_3$ data with superimposed variability were used to create a gridded map of $\%CaCO_3$. The best estimate of $\%CaCO_3$ at each grid point was taken to be the mean overall Monte Carlo simulations, and the sensitivity of the MAR estimate to $\%CaCO_3$ uncertainty was derived from the variation in calculated regional MAR between the Monte Carlo simulations (Table 3).

The uncertainty in the mean non-$CaCO_3$ mass accumulation rate was estimated from the variance of the data in Appendix A2. Confidence limits for our estimate of the mean can be estimated from the variance of a small sample to be

$$\text{c.l.}_{\text{mean non CaCO}_3\text{ MAR}} = \pm t_c \frac{s}{\sqrt{n}}$$

where s is the square root of the variance s^2 and t_c is the critical cutoff value for the Student's t distribution with n-1 degrees of freedom. Division by root n converts the scatter in the data to the uncertainty in the mean value of the data. For

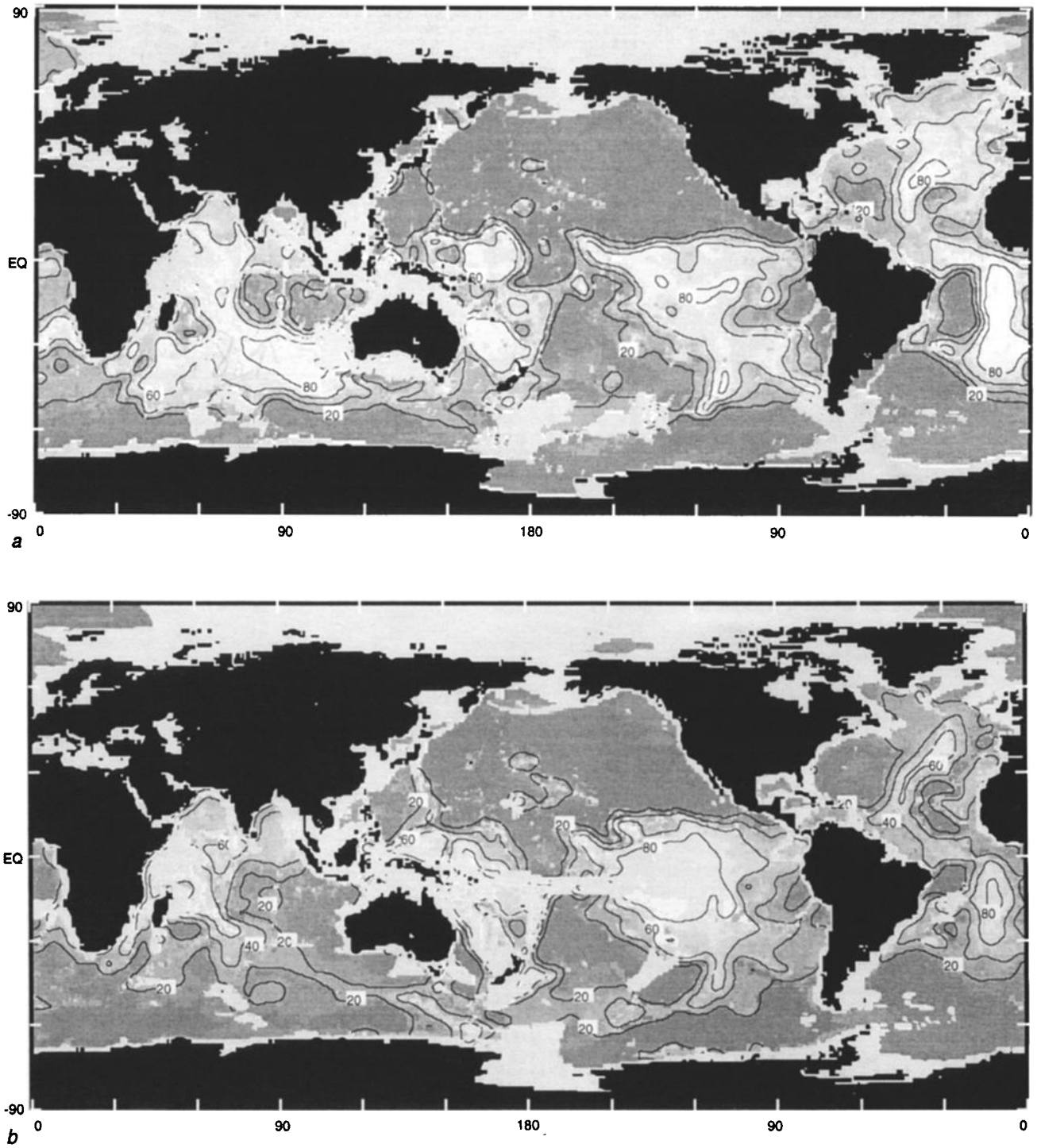

Figure 8. Gridded maps of %$CaCO_3$ (a) in core-top sediments and (b) during the last glacial maximum. The contour interval is 20%. Higher LGM $CaCO_3$ concentrations are found in equatorial Pacific sediments, while concentrations in the Atlantic, Indian, and Southern Oceans are lower.

propagation of the uncertainty to the final answer we can estimate the variance of the mean, σ^2_{mean}, as

$$\sigma^2_{mean} = \left(\frac{t_c}{z_c}\right)^2 \frac{s^2_{sample}}{n} \quad (2)$$

where $z_c = 1.96$ for a 95% two-sided normal distribution. The relative confidence level estimates vary widely by region and time period (Table 2).

The total uncertainty in the regional estimates of $CaCO_3$ MAR is derived from a combination of uncertainty in the non-

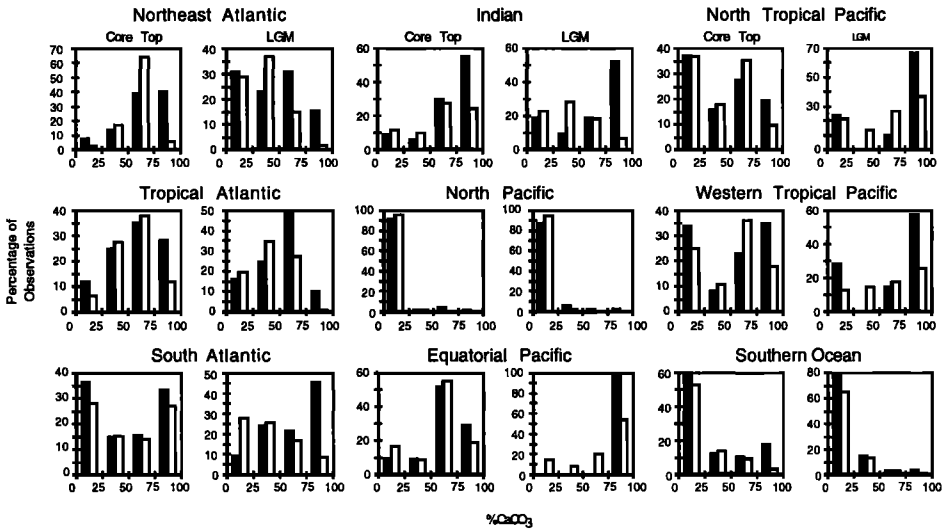

Figure 9. The distribution of $CaCO_3$ concentrations in the ungridded data and in the gridded maps plotted as histograms by region. Solid bars are ungridded data; open bars are gridded values.

$CaCO_3$ MAR and from the %$CaCO_3$ field (the two factors on the right-hand side of (1). These uncertainties are combined as

$$\frac{\sigma^2_{\text{regional CMAR}}}{\text{CMAR}_{\text{best}}} = \frac{\sigma^2_{\text{non-CaCO}_3\text{ MAR}}}{\text{mean}_{\text{non-CaCO}_3\text{ MAR}}} + \frac{\sigma^2_{\%\text{CaCO}_3\text{ map}}}{\text{mean}_{\text{Monte Carlo simulations}}}$$

where $\text{CMAR}_{\text{best}}$ is the regional estimate of $CaCO_3$ MAR using the mean value of the non-$CaCO_3$ MAR and the best map of %$CaCO_3$. Most of the uncertainty in the CMAR estimate derives from uncertainty in the mean non-$CaCO_3$ MAR value (Table 3). The uncertainty in the sum of the CMAR values in all of the regions (as close as we can get with current data to a global estimate) comes from

$$\sigma^2_{\text{sum}} = \sigma^2_{\text{region1}} + \sigma^2_{\text{region2}} + \ldots$$

where the regional and summed values of σ can be used to estimate 95% confidence limits for CMAR as

$$\text{c.l.}_{95\%} = \pm 1.96\ \sigma$$

The uncertainties in our final estimates vary by region depending on how much MAR data exist in each area (Table 4). The uncertainties are fairly high in some regions, but this situation will improve with more MAR data in the future.

4. Results and Discussion

The analysis shows higher calcite burial during LGM in the Pacific (consistent with *Farrell and Prell* [1989]) and North

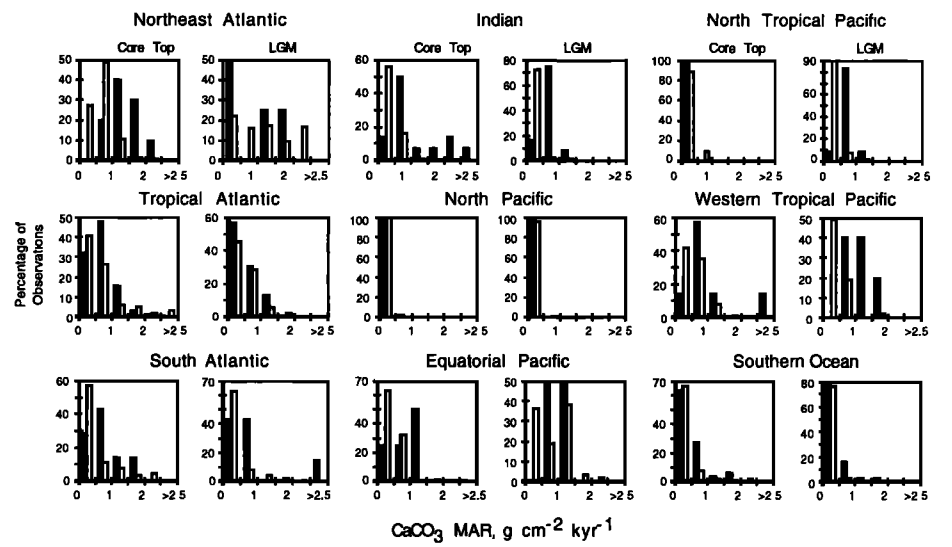

Figure 10. A comparison of the distribution of MAR values in the ungridded data with the gridded results of the constant dilution assumption method using the best maps of %$CaCO_3$. The binning interval is 0 5 g cm^{-2} kyr^{-1}. Solid bars are ungridded data; open bars are gridded values.

Table 3. Statistics of Gridded MAR Calculation

Region	Holocene			Last Glacial Maximum		
	Best MAR[a]	Mean MAR[b]	Relative Confidence Limits	Best MAR[a]	Mean MAR[b]	Relative Confidence Limits
NE Atlantic	3.6	3.6	8%	5.2	5.1	8%
East Equatorial Atlantic	10.4	10.3	2%	7.3	7.6	9%
South Atlantic	10.8	9.7	4%	6.8	6.7	10%
Indian Ocean	6.8	7.5	8%	3.6	4.8	21%
North Pacific	0.1	0.2	52%	0.7	0.9	42%
Equatorial Pacific	2.1	2.1	13%	4.1	3.9	13%
North Equatorial Pacific	1.4	1.5	16%	2.2	2.3	16%
Western Tropical Pacific	4.4	4.6	8%	2.4	3.0	27%
Southern Ocean	18.0	18.2	2%	11 4	12.4	7%

[a]Estimate derived from the "best" map of $\%CaCO_3$ (a grid of mean values of $\%CaCO_3$ over all Monte Carlo simulations).
[b]Mean of all CMAR values from 100 Monte Carlo simulations.

Atlantic regions and lower burial in the tropical and South Atlantic, the Indian, and the Southern Oceans (Figure 11). The Indian Ocean result is dominated by an apparent northward shift in low-calcite Southern Ocean sediments. Overall, the total burial rate over all regions was slightly lower during LGM. The analysis is slightly biased toward lower LGM rates because of a greater area of missing $\%CaCO_3$ gridded estimates from LGM, but the area-specific calcite burial is also lower during LGM (Table 4), so this effect is small. A more serious bias comes from the South Pacific, where $\%CaCO_3$ was higher during LGM but was neglected from our analysis because of a lack of MAR data. Globally, our analysis covers 67% of the grid points with $\%CaCO_3 > 75\%$ for core-top data, but for LGM the coverage is only 48%. If for the sake of discussion we assume that the $CaCO_3$ burial rate scales with the area of >75% $CaCO_3$ sediments, then we project that our global total should be 8.6×10^{12} mol yr^{-1}, slightly smaller than Milliman's estimate of core-top calcite burial (11×10^{12} mol yr^{-1}) [*Milliman*, 1974; *Milliman*, 1993]. For LGM the scaled up value would be 9.2×10^{12} mol yr^{-1}, suggesting that the apparent decrease in LGM calcite burial in our analysis might be due to a shift to of $CaCO_3$ sediments to the undersampled South Pacific.

Overall, we find no significant change in the global burial rate of $CaCO_3$ in the deep sea between last glacial maximum time and today. This result contradicts expectations based on

Table 4. Summary of Final Regional $CaCO_3$ Mass Accumulation Rate Estimates

Region	Area[a]	Holocene			Last Glacial Maximum		
		Coverage	CMAR[b]	Specific MAR[c]	Coverage	CMAR[b]	Specific MAR[c]
NE Atlantic	5.64	89%	3.6±0.8	0.71	84%	5.2±3.4	1.11
Tropical Atlantic	17.60	84%	10.4±0.8	0.71	82%	7.3±1.9	0.51
South Atlantic	27.20	84%	10.8±1.5	0.47	77%	6.8±2.0	0.33
Indian Ocean	30.15	73%	6.8±1.5	0.31	75%	3.6±1.9	0.16
North Pacific	17.07	99%	0.1±0.1	0.01	98%	0.7±0.6	0.04
Equatorial Pacific	5.02	100%	2.1±0.5	0.42	98%	4.1±1.1	0.71
North Equatorial Pacific	8.98	99%	1.4±0.5	0.16	99%	2.2±0.5	0.23
Western Tropical Pacific	10.62	90%	4.4±0.9	0.47	70%	2.4±1.3	0.32
Southern Ocean	78.69	81%	18.0±2.4	0.28	84%	11.4±3.0	0.17
Total			57.6±3.6	0.34 ±.02		43.7±6.0	0.26 ±.03
Area covered, $\%CaCO_3 > 75\%$		67%			48%		
Corrected total			86			91	

[a]Units of 10^6 km^2.
[b]Units of 10^{11} mol $yr^{-1} \pm 1.96\sigma$.
[c]Units of g cm^{-2} kyr^{-1}.

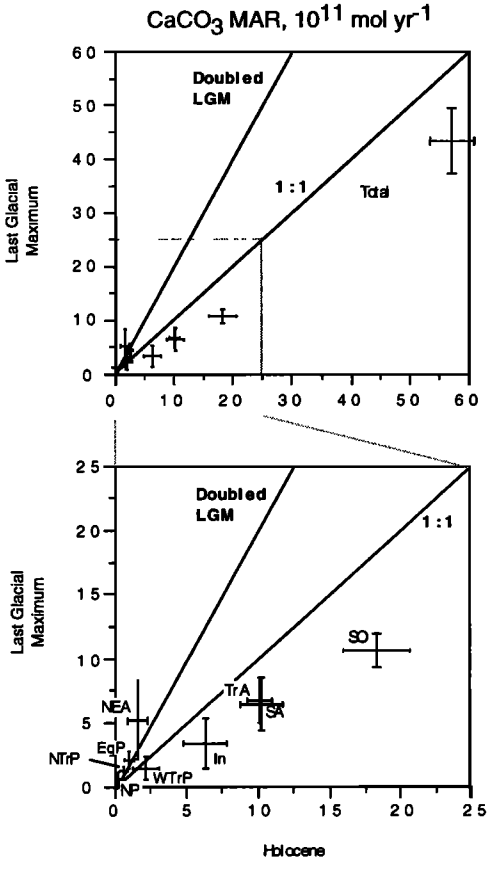

Figure 11. A comparison of Holocene and LGM regional rates of $CaCO_3$ accumulation, where the error bars represent 95% confidence intervals. LGM values are indistinguishable from Holocene values except in the tropical Atlantic and the Indian Oceans, where they are lower, and the equatorial Pacific, where they are higher.

estimates of shallow water deposition rates and an assumption that the ocean was in steady state, which predict that the locus of carbonate burial shifted from the shallow seas to the deep ocean during glacial times. If shallow water deposition accounts for roughly the same scale of $CaCO_3$ burial as the deep sea today [*Milliman*, 1993], and shallow water deposition was significantly less during LGM [*Opdyke and Walker*, 1992; *Milliman*, 1993], then we might expect as much as double the Holocene rate of deep sea $CaCO_3$ deposition during LGM. Possible explanations include (1) the oceans still being out of steady state following the perturbations to the alkalinity cycle in the ocean associated with the glacial termination (coral growth, forest uptake of CO_2, and any change in steady state ocean alkalinity), (2) an LGM weathering rate decrease due to a slower glacial hydrological cycle, (3) LGM shallow water depositions being larger than is generally believed, or (4) estimates of present-day deposition rates may be high. If the rate of shallow water deposition today is lower than is generally believed, then the same relative decrease would be less significant to the global ocean alkalinity budget. Resolution of these issues may require a longer time sequence of deep ocean $CaCO_3$ burial rate estimates and independent estimates of chemical weathering and shallow water $CaCO_3$ deposition.

5. Summary

We attempt to estimate the LGM rate of calcite burial by interpolating measured mass accumulation rate data across variations in $\%CaCO_3$ by assuming the accumulation rate of non-$CaCO_3$ material to be regionally constant and independent of $\%CaCO_3$. Burial rates decreased in the Atlantic and increased in the equatorial Pacific. The sum of the regional MAR estimates is $57.6 \pm 3.5\times10^{11}$ mol yr^{-1} today and $43.7 \pm 6.0\times10^{11}$ mol yr^{-1} during LGM, where uncertainties represent 95% confidence limits. However, only 67% of the present-day area of high-$CaCO_3$ sediments are actually included in regions of adequate MAR data coverage, and 48% of LGM high-$CaCO_3$ sediments. If we normalize these estimates by high-$CaCO_3$ sediment coverage we conclude that the globally integrated burial rate of $CaCO_3$ during LGM was not significantly higher than today (8.6 and 9.2×10^{12} mol yr^{-1}, respectively). The results from this study imply either (1) a non-steady state ocean on timescales of the glacial/interglacial cycles, (2) a glacial decrease in weathering rates, (3) that the rate of shallow water $CaCO_3$ deposition during LGM was comparable to today, or (4) that present-day shallow water deposition today is insignificant relative to deposition in the deep sea.

Acknowledgments. This project was supported by NSF Grant OCE-9521098 and benefitted by discussion with John Milliman and participants of a "Carbonate Symposiom" organized by John Milliman and Andre Droxler.

References

Andrews, J. E., et al., Site 285, in *Initial Reports of the Deep Sea Drilling Project*, vol. 30, 753 pp., U.S. Gov. Print. Off., Washington, D C., 1975.

Archer, D. E., An atlas of the distribution of calcium carbonate in sediments of the deep sea, *Global Biogeochem Cycles, 10*, 159-174, 1996.

Archer, D., H. Kheshgi, and E. Maier-Riemer, Multiple timescales for neutralization of fossil fuel CO_2, *Geophys. Res. Lett., 24*, 405-408, 1997.

Arrhenius, G., Sediment cores from the east Pacific: Properties of the sediments, in *Reports of the Swedish Deep Sea Expedition*, vol. 5, edited by H. Pettersson, Elanders, Göteborg, Sweden, 1952.

Balsam, W. L., Late quaternary sedimentation in the western North Atlantic: Stratigraphy and paleoceanography, *Palaeogeogr. Palaeoclimatol. Palaeoecol., 35*, 215-240, 1981.

Balsam, W., and F. McCoy, Atlantic sediments: Glacial/interglacial comparison, *Paleoceanography, 2*, 531-542, 1987.

Bareille, G., Flux Sedimentaires: Paleoproductivité et Paleocirculation de l'Océan Austral au cours des 150,000 dernières années, Ph. D. thesis, 259 pp.,Univ. de Bordeaux, Bordeaux, France, 1991.

Barker, P. F., et al., *Initial Reports of the Deep Sea Drilling Project*, vol. 113, 785 pp., U.S. Gov. Print. Off., Washington, D. C., 1988.

Barron, J., B. et al., *Proceedings of the Ocean Drilling Program, Initial Reports*, vol. 113, 939 pp., Ocean Drill. Program, College Station, Texas, 1989.

Berger, W. H., Deep-sea carbonates: Pleistocene dissolution cycles, *J. Foraminiferal Res., 3*, 187-195, 1973.

Berger, W. H., Deglacial CO_2 buildup:

Constraints on the coral reef model, *Palaeogeogr. Palaeoclimatol. Palaeoecol., 40*, 235-253, 1982.

Berger, W. H. and J. S. Killingley, Box cores from the equatorial Pacific: ^{14}C sedimentation rates and benthic mixing, *Mar. Geol., 45*, 93-125, 1982.

Berger, W. H., J. C. G. Adelseck, and L. A. Mayer, Distribution of carbonate in surface sediments of the Pacific Ocean, *J. of Geophys. Res., 81*, 2617-2627, 1976.

Biscaye, P. E., V. Kolla, and K. K. Turekian, Distribution of calcium carbonate in surface sediments of the Atlantic Ocean, *J. Geophys. Res., 81*, 2592-2603, 1976.

Boyle, E. A., Cadmium: Chemical tracer of deepwater paleoceanography, *Paleoceanography, 3*, 471-489, 1988.

Broecker, W. S., and T. H. Peng, *Tracers in the Sea*, 690 pp., Lamont-Doherty Earth Observatory, Palisades, N. Y., 1982.

Broecker, W. S. and T. Takahashi, Calcium carbonate precipitation on the Bahama Banks, *J. of Geophys. Res., 71*, 1575-1602, 1966.

Broecker, W. S., M. Klas, E. Clark, E. Bonani, S. Ivy, and W. Wolfi, The influence of $CaCO_3$ dissolution on core-top radiocarbon ages for deep-sea sediments, *Paleoceanography, 6*, 593-608, 1991.

Burkle, L. H., D. B. Clarke, and N. J. Shackleton, Isochronous last-abundant-appearance datum (LAAD) of the diatom Hemidiscus karsteni in the Sub-Antarctic, *Geology, 6*, 243-246, 1978.

Burns, R. E., et al., *Initial Reports of the Deep Sea Drilling Project*, vol. 21, 931 pp., U.S. Gov. Print. Off., Washington, D. C., 1973.

Charles, C. D., P. N. Froelich, M. A. Zibello, R. A. Mortlock, and J. J. Morley, Biogenic opal in Southern Ocean sediments over the last 450,000 years: Implications for surface water chemistry and circulation, *Paleoceanography, 6*, 697-728, 1991.

Ciesielski, P. F., et al., *Proceedings of the Ocean Drilling Program, Initial Reports*, vol. 114, 815 pp., Ocean Drilling Program, College Station, Texas, 1988.

Cooke, D. W. and J. D. Hays, Estimates of Antarctic Ocean seasonal sea-ice cover during glacial intervals, in *Antarctic Geoscience*, edited by C. Craddock, pp. 1017-1025, Univ. of Wis. Press, Madison, 1982.

Creager, J. S., et al., *Initial Reports of the Deep Sea Drilling Project*, vol. 19, 913 pp., U.S. Gov. Print. Off., Washington, D. C., 1973.

Cremer, M., J.-C. Faugeres, F Grousset, and E. Gonthier, Late Quaternary sediment flux on sedimentary drifts in the northeast Atlantic, *Sediment. Geol., 82*, 89-101, 1993.

Curry, W. B., and G. P. Lohmann, Late Quaternary carbonate sedimentation at the Sierra Leone Rise (eastern equatorial Atlantic), *Mar. Geol., 70*, 223-250, 1986.

Curry, W. B , and G. P. Lohmann, Reconstructing past particle fluxes in the tropical Atlantic Ocean, *Paleoceanography, 5*, 487-506, 1990.

Cwienk, D. S., Recent and glacial-age organic carbon and biogenic silica accumulation in marine sediments, M. S. thesis, 237 pp., Univ. of R. I., Kingston, 1986.

Davies, T. A., et al., *Initial Reports of the Deep Sea Drilling Project*, vol. 26, 1129 pp., U.S. Gov. Print. Off., Washington, D. C., 1974.

Droxler, A. W., G. A. Haddad, D. A. Mucciarone and J. L. Cullen, Pliocene-Pleistocene aragonite cyclic variation in Holes 714a and 716b (the Maldives) compared with Hole 633a (the Bahamas): Records of climate induced $CaCO_3$ preservation at intermediate water depths, *Proc. Ocean Drill. Program Sci. Results, 115* 539-576, 1990.

Emerson, S. R. and D. E. Archer, Glacial carbonate dissolution cycles and atmospheric pCO_2: A view from the ocean bottom, *Paleoceanography, 7*, 319-332, 1992.

Farrell, J. W., $CaCO_3$ accumulation in the central equatorial Pacific during the late Quaternary, Ph. D. thesis, 512 pp., Brown Univ., Providence, R. I., 1990.

Farrell, J. W., and W. L. Prell, Climate change and $CaCO_3$ preservation: An 800,000 year bathymetric reconstruction from the central equatorial Pacific Ocean, *Paleoceanography, 4*, 447-466, 1989.

Francois, R., and M. P. Bacon, Variations in terrigenous input into the deep equatorial Atlantic during the past 24,000 years, *Science, 251*, 1473-1476, 1991.

Hayes, D. E., et al., *Initial Reports of the Deep Sea Drilling Project*, vol. 28, 1017 pp., U.S. Gov. Print. Off., Washington, D. C., 1975.

Hays, J. D., J. A. Lozano, N. Shackleton, and G. Irving, Reconstruction of the Atlantic and western Indian ocean sectors of the 18,000 B. P. Antarctic Ocean, in *Investigation of Late Quaternary Paleoceanography and Paleoclimatology*, edited by R. Cline and J. D. Hays, *Geol. Soc. of Am. Mem., 145*, 337-372, 1976.

Heath, G. R., et al., *Initial Reports of the Deep Sea Drilling Project*, vol. 86, 804 pp., U.S. Gov. Print. Off., Washington D. C., 1982.

Heezen, B. C., et al., *Initial Reports of the Deep Sea Drilling Project*, vol. 20, 958 pp., U.S. Gov. Print. Off., Washington, D. C., 1973.

Howard, W. R., and W. L. Prell, Late Quaternary surface circulation of the southern Indian Ocean and its relation to orbital variations, *Paleoceanography, 7*, 79-118, 1992.

Howard, W. R. and W. L. Prell, Late Quaternary $CaCO_3$ production and preservation in the Southern Ocean: Implications for oceanic and atmospheric carbon cycling, *Paleoceanography, 9*, 453-482, 1994.

Hussong, D. M., et al., *Initial Reports of the Deep Sea Drilling Project*, vol. 60, 929 pp., U.S. Gov. Print. Off., Washington, D. C., 1981.

Imbrie, J., J. D. Hays, D. G. Martinson, A. McIntyre, A. C. Mix, J. J. Morley, N. G. Pisias, W. L. Prell, and N. J. Shackleton, The orbital theory of Pleistocene climate: Support from a revised chronology of the marine $\delta^{18}O$ record, in *Milankovitch and Climate*, edited by A. L. Berger et al., pp. 269-305, D. Riedel, Hingham, Mass , 1984.

Karig, D. E., et al., *Initial Reports of the Deep Sea Drilling Project*, vol. 31, 926 pp., U.S. Gov. Print. Off., Washington, D. C., 1975.

Karlin, R., M. Lyle, and R. Zahn, Carbonate variations in the northeast Pacific during the late Quaternary, *Paleoceanography, 7*, 43-61, 1992.

Keigwin, L. D., G. A. Jones, and P. N. Froelich, A 15,000 year paleoenvironmental record from Meiji seamount, far northwestern Pacific, *Earth Planet. Sci. Lett, 111*, 425-440, 1992.

Keir, R. S., and W. H. Berger, Late Holocene carbonate dissolution in the equatorial pacific: Reef growth or neoglaciation?, in *The Carbon Cycle and Atmospheric CO_2: Natural Variations Archean to Present, Geophys. Monogr. Ser.*, vol. 32, edited by E. T. Sundquist and W. S. Broecker, AGU., Washington, D. C., 1985.

Kent, D. V., Apparent correlation of paleomagnetic intensity and climatic records in deep-sea sediments, *Nature, 299*, 538-539, 1982.

Kolla, V., A. W. H. Be, and P. E. Biscaye, Calcium carbonate distribution in the surface sediments of the Indian ocean, *J. Geophys. Res., 81*, 2605-2616, 1976.

LaMontagne, R. W., R. W. Murray, K.-Y. Wei, M. Leinen, and C.-H. Wang, Decoupling of carbonate presevation, carbonate concentration, and biogenic accumulation: A 400-kyr record from the central equatorial Pacific Ocean, *Paleoceanography, 11*, 553-563, 1996.

Larson, R. L., et al., *Initial Reports of the Deep Sea Drilling Project*, vol. 32, 980 pp., U.S. Gov. Print. Off., Washington, D C., 1975.

Leinen, M., Calcium carbonate sedimentation at subtropical South Pacific drill sites from Leg 92 and the carbonate stratigraphy of Site 598: Preliminary studies, edited by M. Leinen et al., *Initial Rep. Deep Sea Drill. Proj., 92*, 305-330, 1985.

Luz, B., Late Pleistocene paleoclimates of the South Pacific based on statistical analysis of planktonic foraminifers, *Palaeogeogr. Palaeoclimatol. Palaeoecol., 22*, 61-78, 1977.

Luz, B., and N. J. Shackleton, $CaCO_3$ solution in the tropical east Pacific during the past 130,000 years, in *Dissolution of Deep-Sea Carbonates*, edited by W. V. Sliter, A. W. H. Be, and W. H. Berger, *Spec. Publ. Cushman Found. Foraminiferal Res., 131*, 142-150, 1973.

Lyle, M., D. W. Murray, B. P. Finney, J. Dymond, J. M. Robbins, and K. Brooksforce, The record of late Pleistocene biogenic sedimentation in the

eastern tropical Pacific Ocean, *Paleoceanography, 3*, 39-59, 1988.

Lyle, M., R. Zahn, F. Prahl, J. Dymond, R. Collier, N. Pisias, and E. Suess, Paleoproductivity and carbon burial across the California current: The multitracers transect, 42°N, *Paleoceanography, 7*, 251-272, 1992.

Lynch-Steiglitz, J., A. V. Geen, and R. G. Fairbanks, Interocean exchange of glacial North Atlantic intermediate water: Evidence from subantarctic Cd/Ca and carbon isotope measurements, *Paleoceanography, 11*, 191-202, 1996.

Mackensen, A., E. Barrera, and H. W. Hubberen, Neogene circulation in the south Indian Ocean: Evidence from benthic foraminifera, carbonate data and stable isotope analyses (Site 751), edited by J. S. W. Wise et al., *Proc. Ocean Drill. Program Sci. Results, 120*, 867-878, 1992.

McManus, D. A., et al., *Initial Reports of the Deep Sea Drilling Project*, vol. 5, 827 pp., U.S. Gov. Print. Off., Washington, D. C., 1970.

Milliman, J D., *Marine Carbonates*, 375 pp., Springer-Verlag, New York, 1974.

Milliman, J. D., Production and accumulation of calcium carbonate in the ocean: Budget of non-steady state, *Global Biogeochem. Cycles, 7*, 927-957, 1993.

Moore, T. C, et al., The reconstruction of sea surface temperatures in the Pacific Ocean of 18,000 B. P., *Mar. Micropaleontol., 5*, 215-247, 1980.

Morley, J. J., and J. D. Hays, Comparison of glacial and interglacial oceanographic conditions in the South Atlantic from variations in calcium carbonate and radiolarian distributions, *Quat. Res., 12*, 396-408, 1979.

Morley, J. J., and N. J. Shackleton, The effect of accumulation rate on the spectrum of geologic time series: Evidence from two South Atlantic sediment cores, in *Milankovitch and Climate*, edited by A. L. Berger et al, pp. 467-480, D. Riedel, Norwell, Mass., 1984.

Mortlock, R. A., C. D. Charles, P. N. Froelich, M. A. Zibello, J. Saltzman, J. D. Hays, and L. H. Burkle, Evidence for lower productivity in the Antarctic Ocean during the last glaciation, *Nature, 351*, 220-223, 1991.

Murray, R., M. Leinen, and A. R. Isern, Biogenic flux of Al to sediment in the central equatorial Pacific Ocean: Evidence for increased productivity during glacial periods, *Paleoceanography, 8*, 651-670, 1993.

Opdyke, B. N., and J. C. G. Walker, Return of the coral reef hypothesis: Basin to shelf partitioning of $CaCO_3$ and its effect on atmospheric pCO_2, *Geology, 20*, 733-736, 1992.

Oritz, J., A. Mix, S. Hostetler, and M. Kashgarian, The California current of the last glacial maximum: Reconstruction at 42°N based on multiple proxies, *Paleoceanography, 12*, 191-206, 1997.

Peterson, L. C., and W. L. Prell, Carbonate dissolution in recent sediments of the eastern equatorial Indian Ocean: Preservation patterns and carbonate loss above the lysocline, *Mar. Geol., 64*, 259-290, 1985.

Prell, W. L., R. E. Marvil, and M. E. Luther, Variablility in upwelling fields in the northwestern Indian Ocean: Two data-model comparison at 9000 years B. P., *Paleoceanography, 5*, 447-457, 1990.

Rea, D K., N. G. Pisias, and T. Newberry, Late Pleistocene paleoclimatology of the central equatorial Pacific: Flux patterns of biogenic sediments, *Paleoceanography, 6*, 227-244, 1991.

Snoeckx, H., and D. K. Rea, Late Quaternary $CaCO_3$ stratigraphy of the eastern equatorial Pacific, *Paleoceanography, 9*, 341-352, 1994.

Steens, N. F., S. Tineke, D. Kroon, W. G. Tenkate, and A. Sprenger, Late Pleistocene periodicities of oxygen isotope ratios, calcium carbonate contents and magnetic susceptibilities of western Arabian sea margin: Hole 728a, edited by W.L. Prell et al., *Proc. Ocean Drill. Program Sci. Results, 117*, 309-320, 1991.

von der Borch, C. C., et al., *Initial Reports of the Deep Sea Drilling Project*, vol. 22, 890 pp., U.S. Gov. Print. Off., Washington, D. C., 1974.

Yang, Y.-L., H. Elderfield, and M. Ivanovich, Glacial to Holocene changes in carbonate and clay sedimentation in the equatorial Pacific ocean estimated from Thorium-230 profiles, *Paleoceanography, 5*, 789-809, 1990.

Yu, E.-F., Variations in the particulate flux of 230-Th and 231-Pa and paleoceanographic applications of the 231-Pa/230-Th ratio, Ph. D thesis, 269 pp., Woods Hole Oceanogr. Inst., Woods Hole, Mass., 1994.

Zahn, R., and T. F. Pedersen, Late Pleistocene evolution of surface and mid-depth hydrography at the Oman margin: Planktonic and benthic isotope records at Site 724, edited by W. L. Prell et al., *Proc. Ocean Drill. Program Sci. Results, 117*, 291-308, 1991.

D. E Archer, Department of Geophysical Sciences, University of Chicago, 5734 South Ellis, Chicago, IL 60637. (e-mail. d-archer@uchicago edu)

N. R Catubig, Museum of Science, 1 Science Park, Boston MA 02114-1099 (e-mail· ncatubig@mos.org)

P de Menocal, Lamont-Doherty Earth Observatory, Palisades, NY 10964 (email peter@ldeo.co umbia.edu)

R Francois, Woods Hole Oceanographic Institution, Woods Hole, MA 02543. (email rfrancois@cliff whoi.edu)

W Howard, Antarctic Cooperative Research Center, University of Tasmania, Hobart, Tasmania 7001, Australia. (email will.howard@utas edu.au)

E -F. Yu, Department of Earth Sciences, National Taiwan Normal University, 88 Section 4 Ting-chou Road, Taipei 117, Taiwan.

(Received March 3, 1997;
revised February 13, 1998;
accepted February 18, 1998)